Terahertz time-domain spectroscopy as a tool to monitor the glass transition in polymers

Steffen Wietzke,[1,*] Christian Jansen,[1] Tilmann Jung,[2] Marco Reuter,[2] Benjamin Baudrit,[3] Martin Bastian,[3] Sangam Chatterjee,[2] and Martin Koch[2]

[1]*Institut für Hochfrequenztechnik, Technische Universität Braunschweig, Schleinitzstrasse 22, 38106 Braunschweig, Germany*
[2]*Fachbereich Physik, Philipps-Universität Marburg,Renthof 5, 35032 Marburg, Germany*
[3]*Süddeutsches Kunststoff-Zentrum, SKZ-KFE gGmbH, Friedrich-Bergius-Ring 22, 97076 Würzburg, Germany*
**steffen.wietzke@ihf.tu-bs.de*

Abstract: We demonstrate the suitability of terahertz time-domain spectroscopy as a non-destructive, contact-free tool to monitor the glass transition in polymers – a core feature of the amorphous phase. Below the glass transition temperature T_g, segmental motions along the polymer chain are frozen due to the lack of free volume between neighboring macromolecules. We show that this transition also reflects in the temperature dependence of the refractive index at terahertz frequencies. Two domains can be identified, which differ in their sensitivity to temperature changes. To verify the proposed approach, we determine the glass transition temperature T_g of semi-crystalline poly(oxymethylene) (POM) with terahertz time-domain spectroscopy and validate the results by destructive differential scanning calorimetry (DSC) measurements.

OCIS codes: (300.6495) Spectroscopy, terahertz; (160.5470) Polymers.

References and links

1. D. Mittleman, ed., *Sensing With Terahertz Radiation* (Springer, Berlin, 2003).
2. P. H. Siegel, "Terahertz technology," IEEE Trans. Microw. Theory Tech. **50**(3), 910–928 (2002).
3. B. M. Fischer, M. Walther, and P. Jepsen, "Far-infrared vibrational modes of DNA components studied by terahertz time-domain spectroscopy," Phys. Med. Biol. **47**(21), 3807–3814 (2002).
4. T. Kleine-Ostmann, R. Wilk, F. Rutz, M. Koch, H. Niemann, B. Güttler, K. Brandhorst, and J. Grunenberg, "Probing noncovalent interactions in biomolecular crystals with terahertz spectroscopy," ChemPhysChem **9**(4), 544–547 (2008).
5. T.-I. Jeon, D. Grischkowsky, A. K. Mukherjee, and R. Menon, "Electrical characterization of conducting polypyrrole by THz time-domain spectroscopy," Appl. Phys. Lett. **77**(16), 2452–2454 (2000).
6. E. Nguema, V. Vigneras, J. L. Miane, and P. Mounaix, "Dielectric properties of conducting polyaniline films by THz time-domain spectroscopy," Eur. Polym. J. **44**(1), 124–129 (2008).
7. Q. Song, P. Han, X.-C. Zhang, C. Zhang, and Y. Zhao, "Temperature dependent terahertz spectroscopy of allopurinol," Int. J. Infrared Millim. Waves **30**, 461–467 (2009).
8. J. Chen, Y. Chen, H. Zhao, G. J. Bastiaans, and X.-C. Zhang, "Absorption coefficients of selected explosives and related compounds in the range of 0.1-2.8 THz," Opt. Express **15**(19), 12060–12067 (2007).
9. B. Fischer, M. Hoffmann, H. Helm, G. Modjesch, and P. U. Jepsen, "Chemical recognition in terahertz time-domain spectroscopy and imaging," Semicond. Sci. Technol. **20**(7), 246–253 (2005).
10. K. Kawase, Y. Ogawa, Y. Watanabe, and H. Inoue, "Non-destructive terahertz imaging of illicit drugs using spectral fingerprints," Opt. Express **11**(20), 2549–2554 (2003).
11. P. F. Taday, "Applications of terahertz spectroscopy to pharmaceutical sciences," Philosoph. Trans. Roy. Soc. A: Math. Phys. Engin. Scie. **362**, 351–364 (2004).
12. C. Jördens, and M. Koch, "Detection of foreign bodies in chocolate with pulsed THz spectroscopy," Opt. Eng. **47**(3), 037003 (2008).
13. N. Krumbholz, T. Hochrein, N. Vieweg, T. Hasek, K. Kretschmer, M. Bastian, M. Mikulics, and M. Koch, "Monitoring polymeric compounding processes inline with THz time-domain spectroscopy," Polym. Test. **28**(1), 30–35 (2009).

#116031 - $15.00 USD Received 1 Sep 2009; revised 23 Sep 2009; accepted 23 Sep 2009; published 6 Oct 2009

14. V. A. Bershtein, and V. A. Ryzhov, "Far infrared spectroscopy of polymers," Adv. Polym. Sci. **114**, 42–121 (1994).
15. N. Naftaly, and R. E. Miles, "Terahertz time-domain spectroscopy for material characterization," in *Proceedings of the IEEE* **95**, 1658–1665 (2007).
16. J. Obradovic, J. H. P. Collins, O. Hirsch, M. D. Mantle, M. L. Johns, and L. F. Gladden, "The use of THz time-domain reflection measurements to investigate solvent diffusion in polymers," Polymer (Guildf.) **48**(12), 3494–3503 (2007).
17. K. Yamamoto, M. Yamaguchi, M. Tani, M. Hangyo, S. Teramura, T. Isu, and N. Tomita, "Degradation diagnosis of ultrahigh-molecular weight polyethylene with terahertz-time-domain spectroscopy," Appl. Phys. Lett. **85**(22), 5194–5196 (2004).
18. J. H. Gibbs, and E. A. DiMarzio, "Nature of the glass transition and the glassy state," J. Chem. Phys. **28**(3), 373–383 (1958).
19. J. M. G. Cowie, ed., *Polymers: Chemistry and Physics of Modern Materials* (Nelson Thornes, Cheltenham, UK, 2001).
20. H. Suzuki, J. Grebowicz, and B. Wunderlich, "Glass Transition of Poly(oxymethylene)," British Polymer J. **17**(1), 1–3 (1985).
21. B. Wunderlich, "Thermodynamics and kinetics of crystallization of flexible molecules," J. Polym. Sci. Part Polym. Phys. **46**(24), 2647–2659 (2008).
22. V. B. F. Mathot, ed., *Calorimetry and Thermal Analysis of Polymers* (Hanser, Munich, 1994).
23. G. Rotter, and H. Ishida, "Dynamic mechanical analysis of the glass transition: curve resolving applied to polymers," Macromolecules **25**(8), 2170–2176 (1992).
24. A. Priyadarshi, L. Shimin, S. G. Mhaisalkar, R. Rajoo, E. H. Wong, V. Kripesh, and E. B. Namdas, "Characterization of optical properties of acrylate based adhesives exposed to different temperature conditions," J. Appl. Polym. Sci. **98**(3), 950–956 (2005).
25. M. Scheller, S. Wietzke, C. Jansen, and M. Koch, "Modelling heterogeneous dielectric mixtures in the terahertz regime: a quasi-static effective medium theory," J. Phys. D Appl. Phys. **42**(6), 065415 (2009).
26. J. Hyun, D. E. Aspnes, and J. J. Cuomo, "Nondestructive measurement of a glass transition temperature at spin-cast semicrystalline polymer surfaces," Macromolecules **34**(8), 2395–2397 (2001).
27. C. Benecke, K. Schmitt, and M. Schadt, "In situ determination of glass transition temperatures in thin polymer films," Liquid Crystals **21**(4), 575–580 (1996).
28. H. Bock, S. Christian, W. Knoll, and J. Vydra, "Determination of the glass transition temperature of nonlinear optical planar polymer waveguides by attenuated total reflection spectroscopy," Appl. Phys. Lett. **71**(25), 3643–3645 (1997).
29. I. Raptis, and C. D. Diakoumakos, "Non-destructive method for monitoring glass transitions in thin photoresist films," Microelectron. Eng. **61–62**, 829–834 (2002).
30. P. Bernazzani, R. F. Sanchez, M. Woodward, and S. Williams, "Determination of the glass transition temperature of thin unsupported polystyrene films using interference fringes," Thin Solid Films **516**(21), 7947–7951 (2008).
31. J. A. Forrest, K. Dalnoki-Veress, J. R. Stevens, and J. R. Dutcher, "Effect of free surfaces on the glass transition temperature of thin polymer films," Phys. Rev. Lett. **77**(10), 2002–2005 (1996).
32. A. Dreyhaupt, S. Winnerl, T. Dekorsy, and M. Helm, "High-intensity terahertz radiation from a microstructured large-area photoconductor," Appl. Phys. Lett. **86**(12), 1–3 (2005).
33. A. Nahata, A. S. Weling, and T. F. Heinz, "A wideband coherent terahertz spectroscopy system using optical rectification and electro-optic sampling," Appl. Phys. Lett. **69**(16), 2321–2323 (1996).
34. D. Grischkowsky, S. Keiding, M. van Exter, and C. Fattinger, "Far-infrared time-domain spectroscopy with terahertz beams of dielectrics and semiconductors," J. Opt. Soc. Am. B **7**(10), 2006 (1990).
35. I. Pupeza, R. Wilk, and M. Koch, "Highly accurate optical material parameter determination with THz time-domain spectroscopy," Opt. Express **15**(7), 4335–4350 (2007).
36. M. Scheller, C. Jansen, and M. Koch, "Analyzing sub-100-µm samples with transmission terahertz time domain spectroscopy," Opt. Commun. **282**(7), 1304–1306 (2009).
37. N. Nagai, and R. Fukasawa, "Abnormal dispersion of polymer films in the THz frequency region," Chem. Phys. Lett. **388**(4-6), 479–482 (2004).

1. Introduction

The terahertz (THz) regime, located between the microwaves and the infrared, is commonly defined by the frequency range of 0.3 THz to 10 THz, i.e., wave numbers of 10 cm^{-1} to 333 cm^{-1}. For long, the lack of efficient THz sources and detectors allowed only small glimpses into this highly interesting but most elusive field of science. Today, the rapid progress in femtosecond laser science and microwave engineering finally enables the full access to this long unexplored frequency band [1,2].

Hence, a plethora of scientific and industrial applications has emerged over the past two decades. Among them are spectroscopy on biomolecules [3,4] and conducting polymers [5,6],

#116031 - $15.00 USD Received 1 Sep 2009; revised 23 Sep 2009; accepted 23 Sep 2009; published 6 Oct 2009

as well as chemical recognition [7–10]. Furthermore, THz technology can prevail as a non-destructive, contactless technique for industrial process monitoring and quality control, e.g., in the pharmaceutical [11], the food [12], and the plastics industry [13].

Altering the chemical composition or the morphology of a polymer, e.g., by ageing or exposition to radiation often results in a change of the dielectric properties. Thus, by monitoring these dielectric parameters using THz time-domain spectroscopy (TDS), information of inter- and intramolecular processes inside the polymer can be obtained. For instance, THz technology has been employed to evaluate the cross-linking process of polystyrene and the epoxy-based photoresist SU-8 [14,15]. Furthermore, the investigation of solvent diffusion in polymers [16] and the degradation diagnosis of ultrahigh-molecular-weight polyethylene [17] have been successfully demonstrated using THz waves. Here, we apply THz TDS as a non-destructive, contact-free tool for the identification of the glass transition temperature of polymers.

The glass transition of polymers is still an active field of discussion. While thermodynamic phase changes always exhibit an equilibrium behavior, the glass transition consists of temperature- and time-dependent relaxations [18]. However, the shape of the steps found in calorimetric curves at the glass transition resembles those of a thermodynamic second-order transition. At the corresponding temperature, discontinuities in the material parameters occur. In amorphous polymers, the long, coiled, entangled macromolecules behave energy-elastic below and entropy-elastic above the glass transition temperature T_g. This phenomenom can be explained by the co-operative chain motions of small backbone segments inside the macromolecule which are frozen below T_g.

An alternate definition of T_g is the concept of the free volume [19]. The free volume is defined as the temperature-dependent space in a polymer sample that is not occupied by the chains due to imperfect packing inside the amorphous domains. As the free volume decreases with falling temperature, there is a critical point at which the remaining space no longer suffices for segmental motions along the polymer chains. The corresponding temperature is referred to as T_g and mainly depends on the chain flexibility, the molecular structure, the molar mass, branching, crosslinking, and the thermal history.

In case of a semi-crystalline polymer like poly(oxymethylene) (POM), only the so-called mobile fraction of the amorphous domains exhibits a glass transition [20]. The crystalline phase and the rigid fraction of the amorphous domains, which is constrained by adjacent crystallites, are not involved in this process. Latter behaves calorimetrically similar to the crystalline phase and remains immobile up to the melting point. More details on the phase structure of semi-crystalline polymers can be found in the work of Wunderlich et al. [21].

Differential scanning calorimetry (DSC) [22] is the prevailing method for the determination of T_g. It detects changes in the heat capacity due the increased mobility of the chain segments above T_g. Depending on the definition of T_g, different points of the DSC curve are employed, such as the onset, the inflection or the end of the calorimetric step. Other methods like the dynamic mechanical analysis (DMA) [23] and the dilatometry [22] consider variations in the mechanical properties and the volume, respectively.

The non-destructive, contact-free technique introduced in this paper indirectly exploits the concept of the free volume by determining the complex refractive index in the THz range as a function of the temperature. As this quantity can be related to the specific volume by the Lorentz-Lorenz law [24] or effective medium theories [25], discontinuities in the thermo-optic coefficient, i.e., the first derivative of the real part of the refractive index n with respect to the temperature T, may serve as an indicator for T_g. Plotting n over T reveals two domains, which differ in the temperature gradient $\partial n/\partial T$: the sensitivity to temperature changes is significantly lower below T_g.

The thermo-optic coefficient of polymers has been investigated by several authors in the infrared, the visible and the UV. The refractive indices were acquired using ellipsometry [26],

#116031 - $15.00 USD Received 1 Sep 2009; revised 23 Sep 2009; accepted 23 Sep 2009; published 6 Oct 2009

prism-coupling schemes (PRS) [24,27], attenuated total reflection spectroscopy (ATR) [28], optical time-domain reflectometry (OTDR) [24], and interferometry [14,29,30].

All the techniques listed above are non-destructive. Yet, they suffer from limitations in determining the refractive index of a sample. When interference fringes from Fourier transform infrared spectroscopy are employed, the temperature-dependent thickness has to be known. Therefore, this method requires an additional measurement step for determining the thickness, which is challenging to realize at low temperatures. ATR and PRS deliver the index of refraction as well as the thickness but a contact to the sample is indispensable. Furthermore, as with ellipsometry, they are able to characterize the surface well, but only thin layers of a material can be investigated. Hence, they cannot provide the bulk glass transition temperature since T_g of a polymer film depends on the material thickness under investigation [29–31]. With OTDR, the backscattered signal is very weak so that averaging a large number of measuring cycles is necessary to achieve an acceptable signal-to-noise ratio. Furthermore, all conventional non-destructive techniques are hard to adapt for low-temperature measurements, limiting their applicability.

In this paper, we introduce THz TDS as a non-destructive, contact-free measuring tool for the accurate determination of the glass transition temperature of polymers. Exemplary, measurements on POM are presented and compared to DSC results. The method is based on the extraction of the refractive index n and the thickness information from a single sample and reference scan. The investigation of polymer transitions at extremely low temperatures becomes possible as THz TDS enables measurements inside a cryostat. Even optically opaque and thick samples can be analyzed due to the high transparency of polymers at THz frequencies. For polymers with a significant amount of amorphous regions or purely amorphous polymers, the THz refractive index and its derivatives with respect to the temperature, such as the thermo-quasi-optic coefficient $\partial n/\partial T$, serve as sensitive indicators for the glass transition temperature.

The remainder of this paper is organized as follows: After an introduction into the experimental setup, the method for extracting the material parameters and the thickness information from the measured THz pulses is presented. Next, the characteristics of the semi-crystalline POM and the DSC results are briefly discussed. Finally, the temperature-dependent dielectric parameters of the sample are investigated to characterize the glass transition.

2. Experimental setup and data analysis

2.1. THz TDS setup

The THz TDS setup is depicted in Fig. 1. The output of a Ti:sapphire femtosecond laser with a pulse width of 50 fs, a repetition rate of 80 MHz and a center frequency of 795 nm is divided into the transmitter and the detector arm using a 70:30 beam splitter (BS).

#116031 - $15.00 USD Received 1 Sep 2009; revised 23 Sep 2009; accepted 23 Sep 2009; published 6 Oct 2009

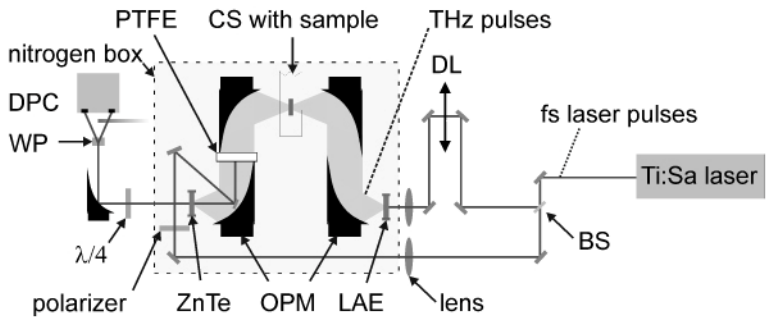

Fig. 1. THz TDS setup with a large-area photoconductor for emission and an electro-optic ZnTe crystal for detection. The cryostat containing the sample between two TPX® windows is transilluminated by the incident THz pulses, which are guided by off-axis parabolic mirrors.

In the transmitter arm, the laser beam is guided to a 25 cm motorized delay line (DL) with a minimum step width of 0.017 µm, which corresponds to 0.22 fs. Afterwards, the beam is focused onto a large-area photoconducting emitter antenna (LAE) [32]. The optically generated carriers in such an emitter are accelerated in an externally applied bias field and THz radiation is emitted. The THz setup is purged with nitrogen gas to minimize the effect of water lines interfering with the results. The THz beam is first collimated and then focused again on the sample by off-axis parabolic mirrors (OPM). To access low temperatures, the measurements were performed in a cryostat (CS). The sample was mounted onto a temperature-controlled cold-finger inside the cryostat with the aid of heat-conducting glue. The cold-finger has a hole of 2 mm in diameter for transmission measurements. It is placed inside the microscopy cryostat MicrostatHe (Oxford Instruments) with two THz-transparent windows made of TPX® (a 4-methylpentene-1-based polyolefin). The cryostat allows for measurements at temperatures down to T = 4.2 K using a continuous helium flux and an insulation vacuum (ca. 10^{-4} Nm^{-2}) with a temperature stability of approximately +/– 0.1 K. The symmetric OPM configuration guides the transmitted THz beam to an electro-optic ZnTe crystal. In this crystal, the polarization of the incident laser beam is changed proportionally to the incoming THz field due to the Pockels effect [33]. A Wollaston Prism (WP) is used to split up both linear polarization components which serve as input to a differential photodiode circuit (DPC). By the stepwise alteration of the delay line position, the entire THz pulse with and without sample in place can be acquired.

Reference measurements with an empty cryostat were performed at the beginning and at the end of the temperature profile scans. At each temperature, a THz pulse transmitted through the sample was acquired. The time between each temperature step was thirteen minutes. The acquisition of the THz pulse took seven minutes. A representative THz reference and sample pulse for POM at T = 200 K are depicted in Fig. 2(a). Compared to the reference scan, the sample pulse is delayed and reduced in amplitude due to the higher refractive index and the inherent absorption of the polymer, respectively. Besides the main pulse, multiple post-echoes are present, arising from reflections at the windows of the cryostat and at other quasi-optical elements. No oscillations due to water vapor are superimposed onto the time-domain signals since the measurement setup was located inside a nitrogen-gas-filled enclosure. The sample pulse contains one additional echo pulse due to the Fabry-Pérot reflection from the sample. It is denoted by an arrow since it plays an important role in the thickness determination as will be discussed later in this paper. Figure 2(b) shows the corresponding Fourier spectra on a logarithmic scale. The superimposed oscillations due to the Fabry-Pérot reflections from the setup elements and the sample are clearly visible. The peak dynamic range is around 66 dB.

#116031 - $15.00 USD Received 1 Sep 2009; revised 23 Sep 2009; accepted 23 Sep 2009; published 6 Oct 2009

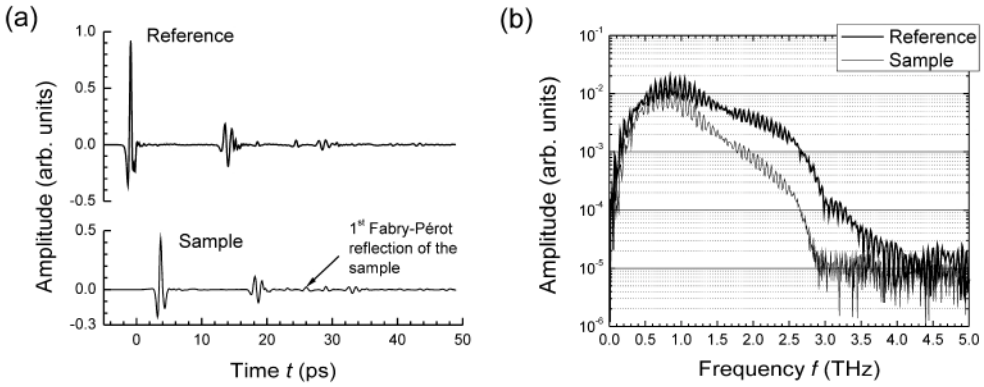

Fig. 2. THz pulses (a) and corresponding Fourier spectra (b) of the reference and the sample scan for POM at $T = 200$ K.

2.2. Data extraction

THz TDS employs a coherent generation and detection scheme. Therefore, this technique has access to both, the phase and the amplitude of the electric field in contrast to far-infrared absorption spectroscopy. Thus, THz TDS is capable of extracting the material's complex refractive index without the need for Kramers-Kronig relations [34].

The data extraction is based on the following principle: First, a theoretical transfer function for the sample under investigation is derived, with the refractive index n, the absorption coefficient α, the sample's thickness L and the number of measured multiple reflections M as free parameters. Now, the approximate number of multiple reflections M is calculated in a preprocessing step, assuming an initial thickness L_0. On this basis, n and α can be computed by a numerical optimization, in which the difference of the theoretical transfer function and the measured one is minimized. However, n and α are still functions of the thickness, which now can be determined, making use of the Fabry-Pérot oscillations of both the measured transfer function and the resulting dielectric material parameters. An additional Fourier transform is applied to the frequency-domain data. The Fabry-Pérot oscillations present on the frequency-domain spectra now appear as discrete peaks. Minimizing the peak amplitude by varying the assumed sample thickness yields the real sample thickness and with it the precise values for n and α. A detailed description of the procedure is given in [35,36].

3. Results and discussion

A bulk sample of commercially available POM with lateral dimensions of 1 cm x 1 cm and a thickness around 920 µm (depending on the temperature) was investigated for this study. On the one hand, the relatively small volume ensures a homogeneous temperature distribution within the sample. On the other hand, this thickness is sufficient to neglect surface phenomena like the decrease of T_g for thin polymer layers [31].

Since the glass transition temperature also depends on the thermal history, the investigation by DSC includes usually a first heating before determining T_g. However, the sample was taken from an injection molded specimen having been produced with a high cooling rate and mechanical stress. Therefore, in order to achieve a representative comparison between the THz TDS measurements without any further thermal preconditioning and the DSC results, no further preheating was applied before the DSC scan. T_g was determined by DSC with a Seiko Instruments' RDC220 using a scanning rate of 10 K/min. Figure 3 shows the DSC results of POM. The glass transition is visible in the measurement curve (heat Q over temperature T) as a step indicating a higher heat capacity above T_g.

#116031 - $15.00 USD Received 1 Sep 2009; revised 23 Sep 2009; accepted 23 Sep 2009; published 6 Oct 2009

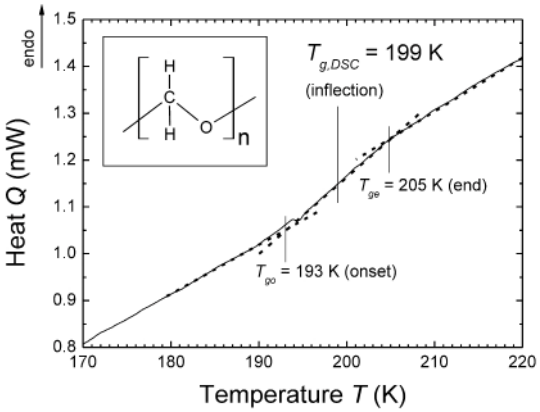

Fig. 3. DSC curve of POM with $T_{g,DSC}$ as the inflection point of the heat step. The inset shows the constitutional repeat unit of this polymer.

The most crucial factor influencing T_g is the chain flexibility. In a polymer such as POM, the bond sequences –(CH_2–O)– can rotate easily (cf. inset Fig. 3). This flexible backbone structure yields a relatively low glass transition temperature. Particularly for semi-crystalline polymers, stating a temperature interval in which the glass transition takes place is preferred to providing a discrete value for T_g: the glass transition is a continous phenomenom rather than a singular event [20,22].

The DSC data shown in Fig. 3 reveals the glass transition in a certain temperature region in which the heat curve deviates from a linear behavior. The onset and the end temperature of this discontinuity are found at T_{go} = 193 K and T_{ge} = 205 K, respectively. The inflection temperature in between is $T_{g,DSC}$ = 199 K. The POM under investigation exhibits a high degree of crystallinity (approximately 56% to 60%). Thus, only the remaining mobile fraction of the amorphous phase contributes to the glass transition and the step in the heat curve is only weakly pronounced.

The THz TDS measurements simultaneously yield the refractive index, the absorption coefficient and the thickness of the sample. The frequency-dependent refractive index and absorption coefficient alpha for a sweep of temperatures are shown in Fig. 4(a) and (b), respectively. An abnormal, temperature-independent dispersion is observed in the refractive index, which arises from the polar nature of POM and has also been reported by Nagai et al. [37]. The refractive index scales with the specific gravity and thus decreases with increasing temperatures. In contrast to that behavior, the absorption coefficient increases towards higher temperatures as it is dominated by the mobility of the molecular chains.

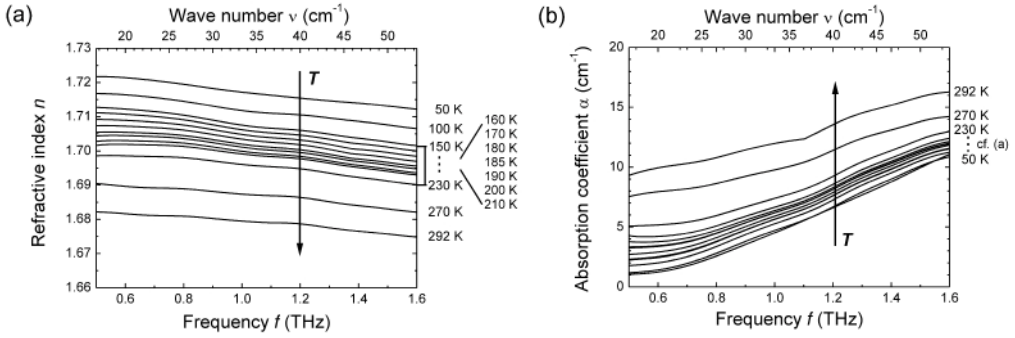

Fig. 4. Frequency-dependent refractive index and absorption coefficient of POM at different temperatures.

#116031 - $15.00 USD Received 1 Sep 2009; revised 23 Sep 2009; accepted 23 Sep 2009; published 6 Oct 2009

Figure 5(a) depicts the refractive index at 1 THz over the temperature for an interval with a higher thermal resolution in the glass transition region. The overall index of refraction decreases with increasing temperature due to the increasing specific gravity. Apart from this generally expected behavior, two domains, one below and one above T_g, are revealed, which differ in the quasi-thermo-optic coefficient $\partial n/\partial T$. In the low temperature domain, the co-operative chain motions are frozen. At temperatures above T_g, additional free volume becomes accessible to the macromolecules of the mobile amorphous fraction allowing crankshaft-like rotations of small backbone segments (Fig. 5(b)). This full mobility yields a higher thermal expansion coefficient, which is tantamount to a stronger decrease in the refractive index with increasing temperature. The intersection of two straight-line segments extrapolating the low- and the high-temperature refractive index regime reveals the expected glass transition at $T_{g,THz}$ = 199 K. This value perfectly agrees with $T_{g,DSC}$, which we derived from Fig. 3, and also with values reported in the literature [20], verifying the reliability of the THz TDS approach.

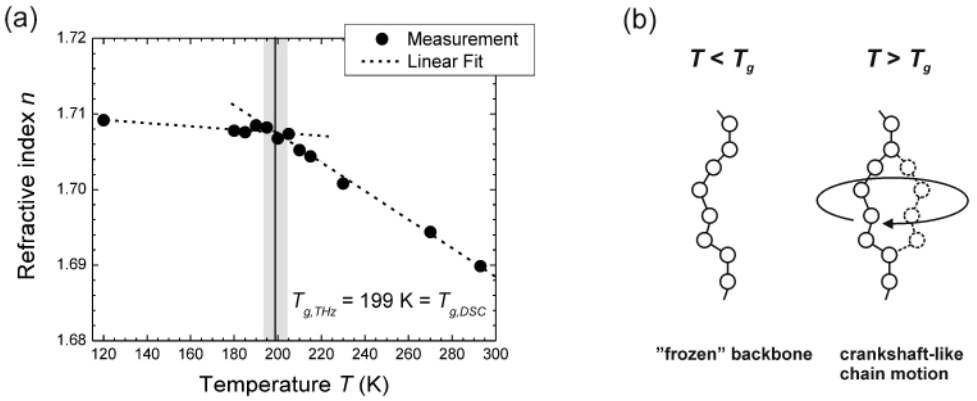

Fig. 5. a) The temperature dependence of the THz refractive index reveals a fractional glass transition of POM at $T_{g,THz}$ = 199 K as the intersection of two linear fits extrapolating the low- and the high-temperature regime. For comparison, the glass transition temperature interval, obtained from DSC measurements (cf. Figure 3), is denoted by the grey area. The values match perfectly. b) Phenomenological visualization of the glass transition.

4. Conclusion

We show that terahertz time-domain spectroscopy can serve as a contactless and non-destructive tool for the monitoring of the glass transition in macromolecules. Freezing of segmental motions in the mobile amorphous fraction below T_g due to the lack of free volume induces a change in the temperature dependence of the refractive index at terahertz frequencies. Semi-crystalline poly(oxymethylene) was investigated both with terahertz spectroscopy and by differential scanning calorimetry. An excellent agreement between the two techniques is achieved verifying the suitability of the proposed approach. In future, terahertz time-domain spectroscopy could also be applied to beta and gamma transitions in polymers enhancing the understanding the glassy state.

Acknowledgements

We gratefully acknowledge the Federal Ministry of Economics and Technology whose budget funds, provided by the Arbeitsgemeinschaft industrieller Forschungsvereinigungen “Otto von Guericke” e.V. (AiF), have supported our work within project number 269ZN. We thank Radoslaw Piesiewicz for providing the poly(oxymethylene). The Marburg group acknowledges financial support by the Federal Ministry of Education and Research (BMBF) and the Optodynamics Research Center. Furthermore, the authors would like to express their gratitude towards W. Dempwolf and H. Menzel (Institut für Technische Chemie, TU

Braunschweig, Germany) as well as towards M. Scheller and T. Grunwald for fruitful discussions. We also thank N. Buchwald, W. Pehlke, O. Flechtner, and D. Kraft for sample preparation and technical assistance, respectively.

#116031 - $15.00 USD Received 1 Sep 2009; revised 23 Sep 2009; accepted 23 Sep 2009; published 6 Oct 2009